

See discussions, stats, and author profiles for this publication at: <https://www.researchgate.net/publication/6452306>

# Rheology of Sodium Hyaluronate Saline Solutions for Ophthalmic Use

ARTICLE in BIOMACROMOLECULES · MAY 2007

Impact Factor: 5.75 · DOI: 10.1021/bm061039k · Source: PubMed

CITATIONS

21

READS

57

6 AUTHORS, INCLUDING:



**Daniela RUSU**

Ecole des Mines de Douai

68 PUBLICATIONS 363 CITATIONS

SEE PROFILE



**H. Burkhard Dick**

Ruhr-Universität Bochum

411 PUBLICATIONS 4,333 CITATIONS

SEE PROFILE



**Bernhard A. Wolf**

Johannes Gutenberg-Universität Mainz

285 PUBLICATIONS 3,419 CITATIONS

SEE PROFILE

# Rheology of Sodium Hyaluronate Saline Solutions for Ophthalmic Use

Daniela Calciu-Rusu,<sup>\*,†</sup> Ernst Rothfuss,<sup>‡</sup> John Eckelt,<sup>†</sup> Tanja Haase,<sup>†</sup>  
H. Burkhard Dick,<sup>§</sup> and Bernhard A. Wolf<sup>†</sup>

*Institut für Physikalische Chemie, Johannes Gutenberg-Universität Mainz, Jakob Welder-Weg 13,  
D-55099 Mainz, Germany, Marienhausklinik St. Elisabeth, Elisabethstr. 1, 66687 Wadern, Germany, and  
Augenklinik, Ruhr-Universität Bochum, In der Schornau 23-25, D-44892 Bochum, Germany*

*Received October 30, 2006; Revised Manuscript Received January 29, 2007*

The aim of this work was to investigate the rheological properties of different saline solutions of sodium hyaluronate (NaHA) with special interest for medical applications. The experimental results were compared with literature data for commercial ophthalmic viscosurgical devices (OVDs) used in cataract surgery. We offer some tools to tailor the rheological behavior of OVDs for different purposes. We have investigated to which extent surgical requirements can be fulfilled by adjusting either the molecular weight of NaHA or its concentration, parameters that are in some respects equivalent but not in others. Furthermore, we demonstrate that moduli and complex viscosities of NaHA saline solutions are adequately falling on master curves, using either empirical or calculated shift factors, the latest ones being based on a modified Rouse model.

## 1. Introduction

Ophthalmic viscosurgical devices (OVDs) are nonactive surgical solutions that have been used for more than 20 years in cataract surgery. The OVDs protect the corneal endothelium during phacoemulsification, preventing trauma caused by contact of the intraocular lens or instruments with the corneal endothelium. Moreover, viscoelastic agents facilitate microsurgical techniques because of their space-maintaining capacity and make the cataract surgery less traumatic.

The class of OVDs available today for cataract and intraocular surgery contains a large variety of polymer solutions, with one or more polymers (sodium hyaluronate, chondroitin sulfate, collagen, hydroxypropylmethylcellulose), and different polymer concentrations and molecular weights, exhibiting a large diversity of physicochemical and rheological properties. However, all OVDs have some common characteristics derived from their intraocular use: they are biocompatible, isotonic, aqueous solutions, and transparent with a well-controlled pH (close to the physiological norm of 7.4).

OVDs can be classified according to their different compositions and physicochemical and rheological behavior. One important criterion is the rheological behavior (i.e., zero-shear viscosity, pseudoplasticity, viscoelastic properties, relaxation time), which influences their suitability for different surgical situations. For instance, the ability of the OVD to maintain space when the ocular tissue is at rest is reflected by the zero-shear viscosity. The resistance offered by the OVD to the normal movement of surgical instruments through the eye depends on the viscosity in the middle-range shear rates ( $1\text{--}10\text{ s}^{-1}$ ). Also, the resistance of OVD to flow through a small cannula is indicated by the viscosity at high-shear rates (about  $10^3\text{ s}^{-1}$ ).<sup>1,2</sup>

Arshinoff proposed a classification<sup>1,3</sup> on the basis of two parameters: zero-shear viscosity and cohesive/dispersive prop-

erties (cohesiveness), considered as describing well enough the OVD behavior during surgery. The cohesiveness of an OVD represents its capability to remain stuck together and to move as a mass, and this characteristic is important not only for its retention in or evacuation from the anterior chamber during phacoemulsification but also in its removal at the end of surgery.<sup>3</sup> Until recently, it was considered that the zero-shear viscosity and the cohesiveness were strongly interconnected and related to the degree of polymer entanglements,<sup>3</sup> and consequently, the zero-shear viscosity was considered to be enough to rank and classify ophthalmic viscoelastic agents. In addition, the zero-shear viscosity also correlates well with the OVD elasticity. With the apparition of new commercial OVDs, on the basis of a combination of polymers, Arshinoff and Jafari expanded the standard classification, considering independently the zero-shear viscosity and cohesiveness.<sup>4</sup>

Clinicians established some surgical requirements for optimum OVD to be used in different moments of the implantation of a foldable intraocular lens (IOL). So, the OVD should have high viscosity and elasticity at low- and medium-shear rates to obtain a deep stable space for the performance of capsulorhexis and, later, to implant the IOL; it should have low viscosity at high-shear rates to be easily injected into the eye through fine cannulas and to maintain reasonable tactile feedback sensation of the injection pressure for the surgeon.<sup>3</sup> The ideal OVD should also present long relaxation times, reflected by the duration of space-occupying effectiveness.<sup>2</sup>

This work is dedicated to the rheological study of saline solutions of sodium hyaluronate (NaHA) for better understanding of the properties of the NaHA-based OVDs and their correlation to the medical requirements. NaHA is the sodium salt of hyaluronic acid, a linear polysaccharide that represents a major component of the extracellular matrix of skin, joints, eye, and many other tissues and organs. Because of the biological specificities and remarkable viscoelastic properties demonstrated by NaHA physiological solutions, they are widely used today in ophthalmology, rheumatology, and dermatology. Furthermore, the medical literature (see references from Dick

<sup>\*</sup> To whom correspondence should be addressed. Tel: +49-6131-39-23118; fax: +49-6131-39-24640; e-mail: daniela.rusu@mines-paris.org.

<sup>†</sup> Johannes Gutenberg-Universität Mainz.

<sup>‡</sup> Marienhausklinik St. Elisabeth.

<sup>§</sup> Ruhr-Universität Bochum.

**Table 1.** Characteristics of the Sodium Hyaluronate Samples Used in This Work

sample	$[\eta]^{25\text{ }^\circ\text{C}}$ mL/g	$M_n$ kg/mol
NaHA450	849	450
NaHA560	1041	560
NaHA650	1167	650
NaHA700	1237	700
NaHA810	1377	810
NaHA850	1418	850
NaHA1100	1739	1100
NaHA1200	1778	1200

and Schwenn<sup>2</sup>) indicates that the commercial OVDs containing NaHA are elected choices in phacoemulsification and extra-capsular cataract.

Several rheological studies<sup>5–13</sup> have investigated the viscoelastic behavior of NaHA aqueous solutions in the absence or the presence of different salts, mainly NaCl, and Cowman and Matsuoka presented an ample overview<sup>14</sup> on this topic. These studies have used NaHA from both animal and fermentation sources in the absence or the presence of proteins. The rheological measurements were performed at different temperatures, most often 25 °C and 37 °C, on different kinds of rheometers, for different polymer concentrations and molecular weights, (mainly 500–2200 kg/mol), and for different solution ionic strengths. Dick and co-workers<sup>2,15</sup> have investigated experimentally the rheological behavior of various commercial OVDs, including the most known NaHA-based OVDs.

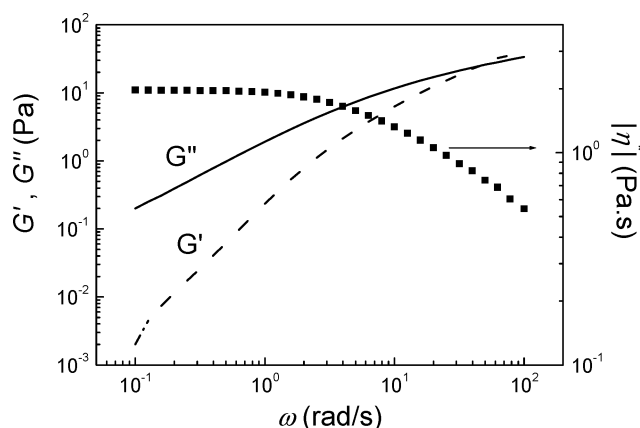
This work presents an experimental rheological study on NaHA saline solutions in different experimental conditions and a systematic comparison with the primary data published on NaHA-based commercial OVDs.<sup>2</sup> Special attention is paid to the relation between the surgical requirements presented earlier and the different classical rheological parameters (e.g., viscosity, dynamic moduli). The possibility of obtaining  $c$ – $T$ – $M$  master curves for the dynamic properties of NaHA solutions is also investigated.

## 2. Experimental Section

**2.1. Materials.** The NaHA samples were obtained by inverse spin fractionation as described elsewhere.<sup>16</sup> Their characteristics are presented in Table 1. The starting material for fractionation (also included in this study) was a sodium hyaluronate from bacterial fermentation, with protein content lower than 0.2%. It was supplied by Synopharm (Charge Nr. 0405A185), and its reported unspecified average molecular weight is 1550 kg/mol, as indicated by the supplier. To preserve a coherence of presentation, the molecular weights of all NaHA samples used in this work were determined by capillary viscometry at 25 °C, using the Kuhn–Mark–Houwink relation. The solvent used for our viscosimetric and rheological measurements is a saline-buffered solution consisting of bidistilled water, 0.146 M NaCl, 0.002 M NaH<sub>2</sub>PO<sub>4</sub>, and 0.0003 M Na<sub>2</sub>HPO<sub>4</sub> (pH  $\approx$  6.1). The different salts were supplied by Fluka (NaCl) and Carl Roth (NaH<sub>2</sub>PO<sub>4</sub>, Na<sub>2</sub>HPO<sub>4</sub>), in p.a. quality.

**2.2. Methods. Preparation of NaHA Solutions.** Before preparing the solutions, the polymer was dried under oil pump vacuum at 50 °C until reaching constant weight. The NaHA solutions were obtained by dissolving the dried polymer and by agitating for 1 day by means of tumble mixer at room temperature. The most concentrated solutions ( $\sim$ 0.03 mg/mL) needed a longer mixing time (up to 3 days). This gentle way of mixing was chosen to avoid degradation of the NaHA, which is sensitive to intense mechanical stress.<sup>16,17</sup>

**Capillary Viscometry.** Viscosimetric measurements were performed at  $25 \pm 0.02$  °C with an automated viscometer (Schott Geräte AVS310, Germany) equipped with Ubbelohde capillary viscometers for dilution

**Figure 1.** Typical frequency sweep measurement.  $c = 0.01$  g/mL NaHA1100;  $T = 20$  °C.

sequences (type I, capillary diameter of 0.63 mm). The measurements were carried out for at least four dilutions per sample. Kinetic energy corrections (Hagenbach corrections) were applied. The intrinsic viscosity,  $[\eta]$ , was determined by using Schulz–Blaschke equation:

$$\frac{\eta_{sp}}{c} = [\eta](1 + k_{SB} \cdot \eta_{sp}) \quad (1)$$

where  $\eta_{sp}$  is the specific viscosity and  $c$  is the polymer concentration (in g/mL). We found a Schulz–Blaschke constant  $k_{SB}^{25^\circ\text{C}} = 0.29 \pm 0.02$ . The molecular weights of all our NaHA samples were calculated using the Kuhn–Mark–Houwink equation,  $[\eta] = K \cdot M^a$ , with  $K = 3.46 \cdot 10^{-2}$  mL/g and  $a = 0.779$ , for NaHA aqueous solutions containing 0.15 M NaCl, at 25 °C.<sup>18</sup>

**Rheometry.** The dynamic measurements were carried out in a TA AR-1000 controlled-stress rheometer (TA Instruments, Inc., United States), using a cone-plate geometry (steel, cone diameter: 20 mm, angle: 1°) and a solvent trap. The measurements were conducted in the linear viscoelastic region, as ensured by independent stress sweep tests. The frequency sweep experiments were performed in the angular frequency range from 0.01 to 100 rad/s and for three temperatures: 10, 20, and 30 °C.

## 3. Results and Discussion

Figure 1 shows the typical dynamic rheological behavior of a NaHA saline solution. The primary data of frequency sweep measurements are complex viscosity  $|\eta^*|$  and dynamic moduli,  $G'$  and  $G''$ , as a function of angular frequency,  $\omega$ . The elastic modulus  $G'(\omega)$  reflects the ability of the polymer system to store elastic energy. In the case of polymer solutions, it depends on the number of interactions (entanglements) and their strength. The greater the number of interactions and the stronger the interaction, the higher is the  $G'(\omega)$  value. The viscous modulus  $G''(\omega)$  is a measure of the flow properties of the polymer system and indicates the unrecoverable viscous loss. It is also related to the number of interactions but is virtually independent of the strength of the interaction. The higher the number of entanglements in which friction can be created, the larger  $G''(\omega)$  is.

The mechanical spectrum, as presented in Figure 1, gives access to the zero-complex viscosity  $|\eta^*|_0$ , by extrapolation, and to the so-called crossover point, which is the intersection point between elastic and viscous moduli curves. It indicates the transition from viscous ( $G' < G''$ ) to elastic ( $G' > G''$ ) behavior of the polymer solutions. Furthermore, the longest relaxation time,  $\tau$ , can be determined as the inverse of the crossover frequency,  $\omega_{\text{crossover}}$ . For ophthalmologic applications of NaHA

**Table 2.** Main Characteristics of the Commercial NaHA-Based OVDs<sup>2</sup> Investigated in This Study<sup>c</sup>

name of the commercial OVD	<i>M</i> kg/mol	<i>c</i> %w	$\eta_0$ Pa·s	$[\eta]$ mL/g	<i>c</i> [η]	( <i>G'</i> = <i>G''</i> ) <sub>crossover</sub> Pa	$\omega_{\text{crossover}}$ rad/s	$\tau^a$ s	$\tau^b$ s
AMO VITRAX	500	3.0	41	952	28.6	287.7	37.810	0.17	0.17
RAYVISC	650	3.0	77	1168	35.0	268.9	19.660	0.32	0.41
AMVISC PLUS	1500	1.6	128	3397	54.4	64.9	2.520	2.50	2.90
DISPASAN	2000	1.0	131	4041	40.4	26.7	1.050	6.00	6.40
VISKO	2000	1.0	206	4041	40.4	20.6	0.400	15.60	10.10
BIOLON	3000	1.0	243	5163	51.6	25.4	0.500	12.60	17.80
VISKO PLUS	3000	1.4	1683	5163	72.3	65.8	0.140	44.60	88.00
HEALON	4000	1.0	243	6143	61.4	19.4	0.290	21.40	23.80
HEALON 5	4000	2.3	5525	6143	141.3	142.4	0.070	87.00	235.00
HEALON GV	5000	1.4	2451	7029	98.4	53.2	0.080	83.00	214.00
ALLERVIS (VISCORNEAL)	5000	1.0	733	7029	70.3	22.2	0.120	50.00	90.00
ALLERVIS (VISCORNEAL) PLUS	5000	1.4	1176	7029	98.4	45.9	0.160	40.00	103.00
MICROVISC	5000	1.0	1163	7029	70.3	24.5	0.068	92.00	142.00
MORCHER OIL	6100	1.0	1253	7926	79.3	26.3	0.069	91.00	187.00
MICROVISC PLUS	7900	1.4	3663	9266	129.7	51.5	0.040	157.00	505.00

<sup>a</sup> Literature data, calculated as  $\tau = 1/\omega_{\text{crossover}}$ . <sup>b</sup> Calculated according to eq 4. <sup>c</sup> *T* = 23 °C.

solutions, both the crossover frequency,  $\omega_{\text{crossover}}$ , and the value of (*G'* = *G''*)<sub>crossover</sub>, indicating the elasticity at  $\omega_{\text{crossover}}$ , are very important.

**3.1. Zero-Shear Viscosity Dependence on *c*, *M*, and *T*.** In the range under investigation, 10–30 °C, the temperature dependence of the viscosity of our NaHA saline solutions obeys the Arrhenius relation:

$$\eta = A \cdot \exp(E_a/RT) \quad (2)$$

where *R* is the universal gas constant (8.314 J/K·mol) and *A* is a system constant. We have found an activation energy *E<sub>a</sub>* = 31–35 kJ/mol, in the same range of values as reported by Gibbs et al. (21–42 kJ/mol).<sup>5</sup> For comparing our rheological results with OVDs' literature data obtained at 23 and 25 °C, the viscosities of our NaHA samples at these two temperatures were calculated using eq 2. The main characteristics of the commercial OVDs included in this work are presented in Table 2.<sup>2</sup>

In the following, we have considered that the empirical Cox–Merz rule is valid for NaHA saline solutions, at least in the range of molecular weights and concentrations under investigation in this work. The Cox–Merz rule assumes that the complex viscosity at a given frequency is equal to the (steady) viscosity at a shear rate numerically equal to the frequency. Consequently, we assumed that the complex viscosity extrapolated at very low frequencies is equal to the zero-shear viscosity,  $|\eta^*|_0 = \eta_0$ . Figure 2a shows on the same plot the zero-complex viscosity for our NaHA solutions and the zero-shear viscosity for different commercial OVDs as a function of the Bueche parameter (*cM*). This parameter is proportional to the number of intermolecular contacts per molecule and controls the rheological properties of concentrated solutions. One can see from the figure that all the data are coherent, and the zero-complex viscosities and zero-shear viscosities are in good agreement, as expected from the Cox–Merz rule. Besides, we found that the zero-shear viscosity depends on (*cM*)<sup>3.4±0.1</sup>. The high dependence of  $\eta_0 \propto M^{3.4}$  is due to the molecular entanglements and has been reported in the literature for a great number of polymers.<sup>19</sup>

Another way to point out the effect of polymer concentration and molecular weight on the zero-shear viscosity of NaHA solutions is to plot the specific viscosity  $\eta_{\text{sp}}$  versus the coil overlap factor, *c*[η], as shown in Figure 2b. The intrinsic viscosities for commercial NaHA-based OVDs were estimated by using the Kuhn–Mark–Houwink parameters<sup>20</sup> for NaHA solutions in 0.15 M NaCl, at 37 °C, and by applying appropriate temperature correction, calculated from our own experimental

data. The molecular weights were used as given by manufacturers. For the sake of comparison, the estimated intrinsic viscosity for HEALON, at 25 °C, is consistent with the one reported in the literature.<sup>9</sup>

For solutions with *c*[η] > 1, the specific viscosity in the Newtonian region was calculated as  $\eta_{\text{sp}} = \eta_0/\eta_{\text{solvent}} - 1$ . Figure 2b points out that all the experimental data and OVDs' literature data are well described by the polynomial equation proposed by Berriaud et al.:<sup>7</sup>

$$\eta_{\text{sp}} = c[\eta] + 0.42 \cdot (c[\eta])^2 + 0.00777 \cdot (c[\eta])^{4.18} \quad (3)$$

So, eq 3 appears to be valid for a wide range of overlap factors *c*[η], up to 140, corresponding in this case to molecular weights up to 7900 kg/mol and polymer concentrations from 1·10<sup>−4</sup> to 3·10<sup>−2</sup> g/mL.

As one can also see in Figure 2b, the commercial OVDs have coil overlap factors ranging from 28 to 150. These *c*[η] values are achieved by using NaHA with very high molecular weight and reasonable concentration (i.e., MICROVISC PLUS, 7900 kg/mol, 0.01 g/mL) or by using relatively low molecular weight NaHA and a high concentration (as in the case of AMO VITRAX, 500 kg/mol, 0.03 g/mL) or by looking for a balance between the NaHA molecular weight and its concentration. One may remark that the most appreciated NaHA-based OVDs from surgery viewpoint<sup>1,2,4,15</sup> are polymer solutions with extremely high overlap factor, *c*[η] ≥ 100.

**3.2. Crossover Point Dependence on *c*, *M*, and *T*.** Figure 3 presents an example of temperature and molecular weight dependence of the dynamic moduli at the crossover frequency. In the range of 10–30 °C, (*G'* = *G''*)<sub>crossover</sub> does not vary significantly with temperature. Furthermore, the molecular weight of the polymer does not influence (*G'* = *G''*)<sub>crossover</sub>, at least in the range under investigation, 500–6100 kg/mol.

The concentration dependence of dynamic moduli at the crossover frequency is shown in Figure 4. We found that (*G'* = *G''*)<sub>crossover</sub> ∝ *c*<sup>2.1±0.1</sup>*M*<sup>0</sup>, which is in good agreement with de Gennes's theoretical prediction<sup>19</sup> (*c*<sup>2.25</sup>*M*<sup>0</sup>) and the experimental finding of Milas et al.,<sup>9</sup> (*c*<sup>2.15</sup>*M*<sup>0</sup>), for a narrower *M* range.

Dick and Schwenn<sup>2</sup> point out that from clinicians' point of view, for IOL implantation, OVDs with  $\omega_{\text{crossover}} \leq 1$  rad/s and high (*G'* = *G''*)<sub>crossover</sub> values are especially suitable. Thus, to identify the optimum characteristics of NaHA solutions, corresponding to the two conditions expressed earlier, we plotted in Figure 5 the ratio between the dynamic moduli and the



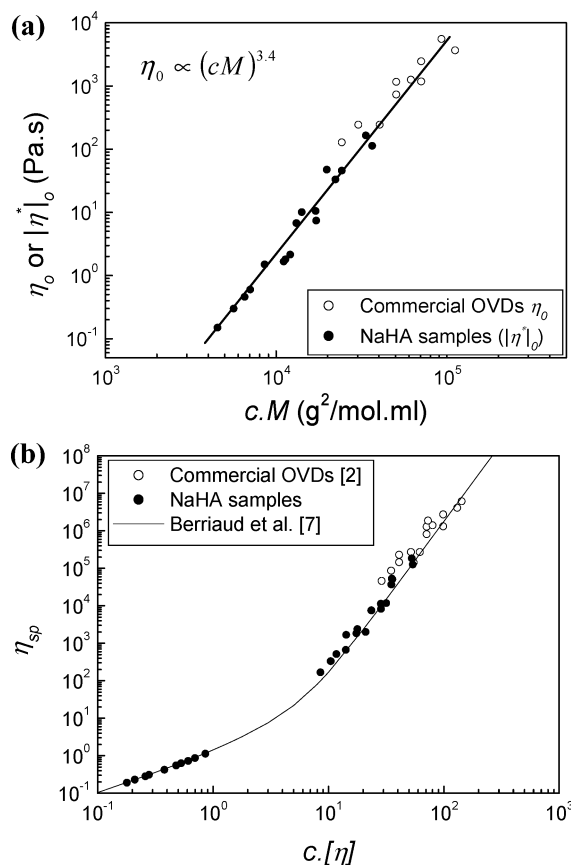


**Figure 2.** Viscosity as a function of (a) Bueche parameter and (b) overlap factor for different NaHA samples.

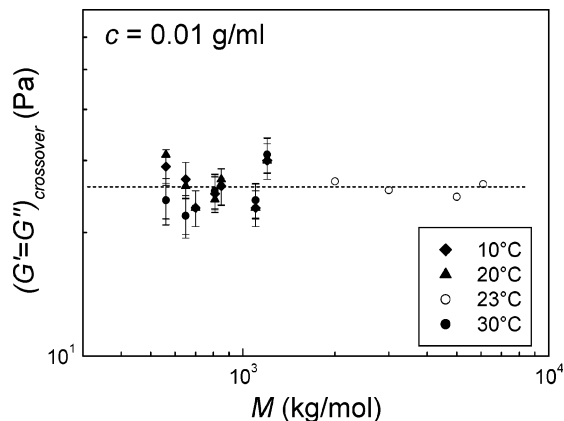


**Figure 3.** Molecular weight and temperature dependence of dynamic moduli at the crossover frequency. Full symbols, our experimental data; open symbols, OVDs' literature data.<sup>2</sup>

frequency at the crossover point,  $(G/\omega)_{\text{crossover}}$ , as a function of the overlap factor. The ratio  $(G/\omega)_{\text{crossover}}$  represents in fact  $(\eta' = \eta'')_{\text{crossover}}$ , where  $\eta'(\omega) = G'(\omega)/\omega$  and  $\eta''(\omega) = G''(\omega)/\omega$  are the real and imaginary parts of the complex viscosity. We obtained a dependence  $(G/\omega)_{\text{crossover}} \propto (c[\eta])^{4.0 \pm 0.1}$ , which justifies quantitatively the previous observation from Figure 2b that the two surgical requirements, high dynamic moduli at the crossover frequency and very low  $\omega_{\text{crossover}}$  (corresponding to large relaxation times), are fulfilled by NaHA-based OVDs with very high overlap factors.

Figure 6 shows the map of dynamic moduli and frequencies at the crossover point for different NaHA samples and commercial OVDs. For a given molecular weight, the larger the polymer concentration, the lower the frequency (higher the

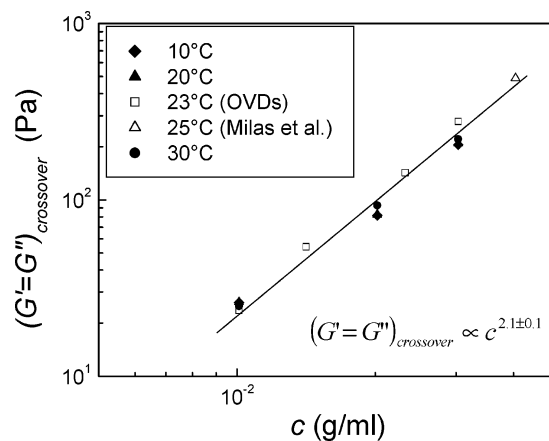


**Figure 4.** Concentration dependence of dynamic moduli at crossover frequency for different NaHA samples. Full symbols, our experimental data; open symbols, literature data: commercial OVDs;<sup>2</sup> the value from Milas et al.<sup>9</sup> corresponds to NaHA solutions with 0.1 M NaCl.

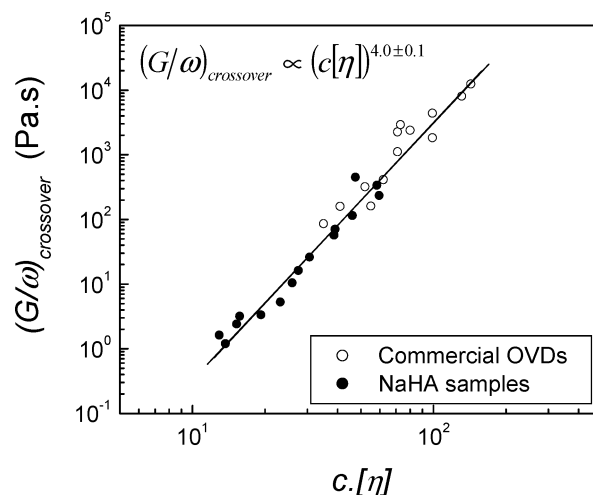


**Figure 5.** The  $(G/\omega)_{\text{crossover}}$  dependence on the overlap factor. Full symbols, our experimental data; open symbols, OVDs' literature data.<sup>2</sup>

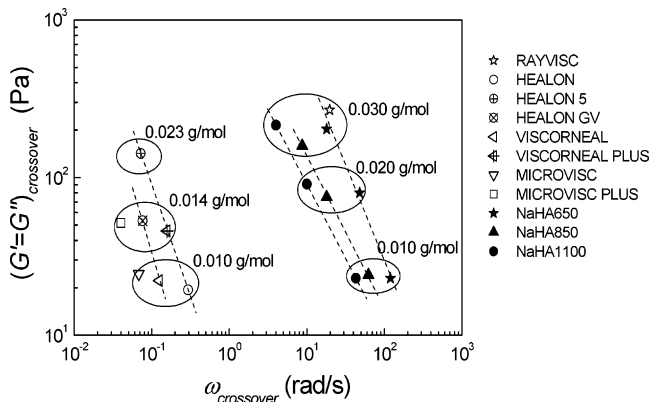


**Figure 6.** Crossover point coordinates for different NaHA solutions. Dashed lines are given to guide the eye and link the solutions on the basis of NaHA with the same molecular weight. Full symbols, our experimental data; open symbols, OVDs' literature data.<sup>2</sup> Data points corresponding to the same concentration of NaHA are visualized by ovals.

relaxation time) is at which the crossover occurs and the higher the elasticity values are at that point. On the other hand, for a given concentration, an increase of the molecular weight induces a decrease of the  $\omega_{\text{crossover}}$  value but has no influence on the elasticity level at the crossover point.

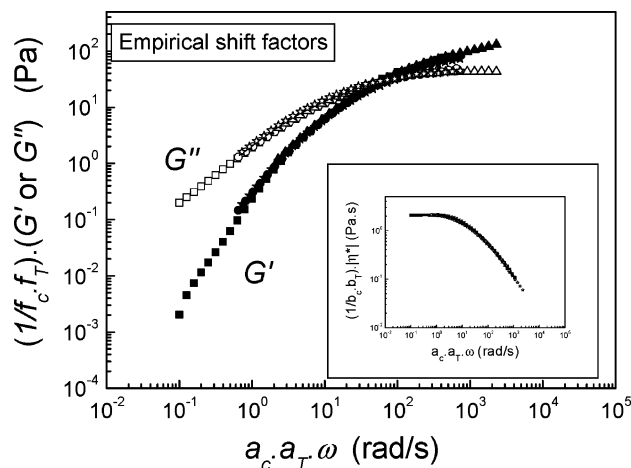


**Figure 7.** Empirical  $c$ - $T$  master curves for NaHA1100. Experimental conditions:  $c = 0.01$ – $0.03$  g/mL;  $T = 10$ – $30$  °C. Reference conditions:  $c_{\text{ref}} = 0.01$  g/mL;  $T_{\text{ref}} = 20$  °C. The insert shows the master curve for the complex viscosity.

We have also investigated the longest relaxation time of our NaHA in saline solutions and commercial OVDs, as obtained from the intersection of  $G'$  and  $G''$  curves, and we compared it with the one indicated by a modified Rouse model:<sup>19,21</sup>

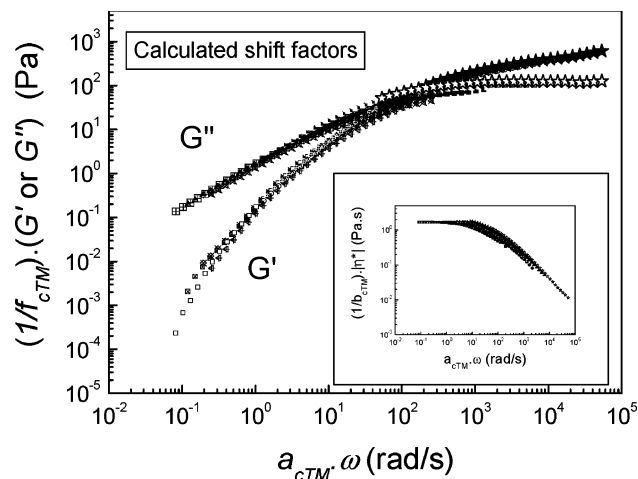
$$\tau = \frac{6M\eta_0}{\pi^2 cRT} \quad (4)$$

Table 2 presents both experimental and calculated values for the relaxation time. A good agreement was generally obtained for commercial OVDs containing NaHA with overlap factors up to around 40. Above these values (except HEALON, with good estimation for  $c[\eta] = 61.4$ ), the calculated relaxation times are typically 1.5–3 times larger than the ones determined via dynamic rheology. This suggests a limit in the application of eq 4 and also may reflect the different molecular weight distributions of NaHA samples ( $M_w/M_n \approx 2.0$ – $3.5$  for our NaHA samples, unknown for the commercial OVDs) and some other differences in the composition of the commercial products.

### 3.3. Time–Temperature–Concentration Master Curves.

Until now, we discussed separately the influence of temperature, polymer concentration, and molecular weight on the dynamic properties of NaHA solutions. In the following, we will investigate the possibility of bringing all the experimental data (dynamic moduli and complex viscosity curves), obtained in different experimental conditions, together into single master curves (one for each rheological parameter), by means of appropriate shift factors.

The idea of  $c$ - $T$  master curves for the complex viscosity and dynamic moduli is based on the method of reduced variables.<sup>21</sup> The model of reduced variables was already applied by Gibbs et al.<sup>5</sup> for studying the effect of temperature, ionic strength, and



**Figure 8.** Calculated  $c$ - $T$ - $M$  master curves for NaHA solutions. Experimental data for NaHA1100, NaHA1200, and NaHA650:  $c = 0.01$ – $0.03$  g/mL;  $T = 10$ – $30$  °C. Star symbols, HEALON:  $c = 0.01$  g/mL;  $T = 23$  °C;  $M = 4000$  kg/mol. Reference conditions:  $c_{\text{ref}} = 0.01$  g/mL;  $T_{\text{ref}} = 25$  °C;  $M_{\text{ref}} = 1100$  kg/mol. The insert shows the master curve for the complex viscosity.

polymer concentration on diluted NaHA saline solutions (concentration  $2 \cdot 10^{-3}$ – $4 \cdot 10^{-3}$  g/mL).

There are different ways to find the shift factors for obtaining a single master curve after choosing the reference conditions: (a) empirically, by shifting the curves until they superpose to the one corresponding to the reference conditions, and (b) by calculating the shift factors according to polymer dynamics theories. One can define three types of shift factors as follows:  $a_j$ , shift in angular frequency;  $f_j$ , shift in dynamic moduli (identical for  $G'$  and  $G''$ ); and  $b_j$ , shift factor for the complex viscosity, where the subscript  $j$  may either refer to  $c$  or  $T$ .

First, we determined the  $c$  and  $T$  shift factors empirically for a given NaHA sample. Figure 7 shows such a family of master curves for solutions of NaHA1100. The empirical temperature-shift factors  $a_T$  and  $b_T$  follow an Arrhenius behavior with the same activation energy  $E_a$  as obtained previously for viscosity. Additionally, we found that the shift factors are interconnected by the following relation:  $b_j = a_j f_j$ , where the subscript  $j$  is either  $c$  or  $T$ .

Next, we investigated the possibility to obtain master curves by calculating the shift factors using the relaxation spectrum from the modified Rouse model:<sup>5,19,21</sup>

$$G_i = \frac{cRT}{M} \text{ and } \tau_i = \frac{6M\eta_0}{\pi^2 i^2 cRT} = \frac{\tau}{i^2}, i = 1, 2, \dots \quad (5)$$

where  $G_i$  and  $\tau_i$  are the modulus contribution and the relaxation time for a model element, and  $\tau$  is the longest relaxation time, as described by eq 4. This time, we calculated the shift factors

**Table 3.** Formulas for Calculating the  $c$ - $T$ - $M$  Shift Factors

parameter to be shifted	$c$ - $T$ - $M$ shift factor
angular frequency	$a_{cTM} = \frac{\tau_i(c, T, M)}{\tau_i(c_{\text{ref}}, T_{\text{ref}}, M_{\text{ref}})} = \frac{\eta_0(c, T, M) \cdot c_{\text{ref}} \cdot T_{\text{ref}} \cdot M}{\eta_0(c_{\text{ref}}, T_{\text{ref}}, M_{\text{ref}}) \cdot c \cdot T \cdot M_{\text{ref}}}$
dynamic moduli $G'$ and $G''$	$f_{cTM} = \frac{G_i(c, T, M)}{G_i(c_{\text{ref}}, T_{\text{ref}}, M_{\text{ref}})} = \frac{c \cdot T \cdot M_{\text{ref}}}{c_{\text{ref}} \cdot T_{\text{ref}} \cdot M}$
(complex) viscosity	$b_{cTM} = \frac{\eta_0(c, T, M)}{\eta_0(c_{\text{ref}}, T_{\text{ref}}, M_{\text{ref}})}$

$a_{cTM}$ ,  $b_{cTM}$ , and  $f_{cTM}$  accounting for the cumulated influence of  $c$ ,  $T$ , and  $M$  according to the equations collected in Table 3. Considering these definitions, the empirical relation found previously ( $b_j = a_j \cdot f_j$ ) agrees well with the relationship between the zero-shear viscosity, the long relaxation time, and the plateau modulus ( $\eta_0 = \tau \cdot G_0$ ), as predicted by the linear viscoelastic model.<sup>22</sup>

Figure 8 presents the  $c$ – $T$ – $M$  master curves obtained by means of calculated shift factors for different NaHA samples (one being a commercial OVD). The reference conditions for the master curves are  $T_{\text{ref}} = 25$  °C,  $c_{\text{ref}} = 0.01$  g/mL, and  $M_{\text{ref}} = 1100$  kg/mol. These data do not fall on a common line to the same extent as the data of Figure 7. There are at least two thinkable reasons for that observation. One lies in possible deficiencies of the modified Rouse model and another in experimental uncertainties in  $\eta_0$ ,  $c$ , and  $M$ , resulting in a scattering of the calculated shift factors.

#### 4. Conclusions

We have shown that the typical dependence of the rheological parameters (such as elastic and viscous moduli, complex viscosity, and zero-shear viscosity) on the molecular weight of the polymer and its concentration, on temperature and frequency can be extended into the  $M$  and  $c$  range characteristic for commercial NaHA-based ophthalmic viscosurgical devices. Furthermore, we demonstrated that in the case of NaHA-based OVDs, the surgical requirements concerning  $\eta_0$ ,  $(G' = G'')_{\text{crossover}}$ , and  $\omega_{\text{crossover}}$  are quantitatively reflected by the coil overlap factor  $c[\eta]$ . The higher the  $c[\eta]$ , the higher are both the zero-shear viscosity and the  $(G/\omega)_{\text{crossover}}$ . The molecular weight of NaHA in the formulation of a NaHA-based OVD greatly influences the value of the crossover frequency but practically does not change  $(G' = G'')_{\text{crossover}}$ ; this value depends only on polymer concentration. The longest relaxation times of NaHA-based commercial OVDs compare well with the predictions of the modified Rouse model up to overlap factors of about 40. Above this limit, this model overestimates  $\tau$  in almost all cases.

The results described above offer some tools to tailor the rheological behavior of OVDs for different purposes. As indicated by the present investigation, the NaHA-based OVDs, which are according to medical literature<sup>1,2,4,15</sup> suited best, are characterized by the highest overlap factors. The central variables to obtain an optimum OVD, the molecular weight of the polymer and its concentration, are in some respects equivalent but not in others.

Finally, we have shown that it is possible to obtain satisfactory master curves for the parameters describing the dynamic behavior of NaHA saline solutions,  $G'$ ,  $G''$ , and  $|\eta^*|$ , and not only in an empirical manner but also by means of shift factors calculated by means of the modified Rouse model.

**Acknowledgment.** The financial support of the Innovationstiftung Rheinland-Pfalz is gratefully acknowledged. The authors thank Dr. Andreas Eich for helpful discussions.

#### References and Notes

- (1) Arshinoff, S. A. *J. Cataract Refractive Surg.* **1999**, *25*, 167–173.
- (2) Dick, H. B.; Schwenn, O. *Viscoelasticity in Ophthalmic Surgery*; Springer-Verlag: Berlin, 2000.
- (3) Arshinoff, S. A.; Wong, E. J. *Cataract Refractive Surg.* **2003**, *29*, 2318–2323.
- (4) Arshinoff, S. A.; Jafari, M. J. *Cataract Refractive Surg.* **2005**, *31*, 2167–2171.
- (5) Gibbs, D. A.; Merrill, E. W.; Smith, K. A.; Balazs, E. A. *Biopolymers* **1968**, *6*, 777–791.
- (6) Fouissac, E.; Milas, M.; Rinaudo, M. *Macromolecules* **1993**, *26*, 6945–6951.
- (7) Berriaud, N.; Milas, M.; Rinaudo, M. *Int. J. Biol. Macromol.* **1994**, *16*, 137–142.
- (8) Roure, I.; Rinaudo, M.; Milas, M.; Frollini, E. *Polymer* **1998**, *39*, 5441–5445.
- (9) Milas, M.; Rinaudo, M.; Roure, I.; Al-Assaf, S.; Phillips, G. O.; Williams, P. A. *Biopolymers* **2001**, *59*, 191–204.
- (10) Ambrosio, L.; Borzacchiello, A.; Netti, P. A.; Nicolais, L. *J. Macromol. Sci., Chem.* **1999**, *A36*, 991–1000.
- (11) Borzacchiello, A.; Ambrosio, L. *J. Biomater. Sci., Polym. Ed.* **2001**, *12*, 307–316.
- (12) Krause, W. E.; Bellomo, E. G.; Colby, R. H. *Biomacromolecules* **2001**, *2*, 65–69.
- (13) Gatej, L.; Popa, M.; Rinaudo, M. *Biomacromolecules* **2005**, *6*, 61–67.
- (14) Cowman, M. K.; Matsuoka, S. *Carbohydr. Res.* **2005**, *340*, 791–809.
- (15) Dick, H. B.; Krummenauer, F.; Augustin, A. J.; Pakula, T.; Pfeiffer, N. *J. Cataract Refractive Surg.* **2001**, *27*, 320–326.
- (16) Calciu, D.; Eckelt, J.; Haase, T.; Wolf, B. A. *Biomacromolecules* **2006**, *7* (12), 3544–3547.
- (17) Prieto, J. G.; Pulido, M. M.; Zapico, J.; Molina, A. J.; Gimeno, M.; Coronel, P.; Alvarez, A. I. *Int. J. Biol. Macromol.* **2005**, *35*, 63–69.
- (18) Bothner, H.; Waaler, T.; Wik, O. *Int. J. Biol. Macromol.* **1988**, *10*, 287–291.
- (19) Doi, M.; Edwards, S. F. *The Theory of Polymer Dynamics*; Clarendon Press: Oxford, U.K., 1986.
- (20) Mendichi, R.; Soltes, L.; Schieron, A. G. *Biomacromolecules* **2003**, *4*, 1805–1810.
- (21) Ferry, J. D. *Viscoelastic Properties of Polymers*; 3rd ed.; Wiley: New York, 1980.
- (22) Bird, R. B.; Armstrong, R. C.; Hassager, O. *Dynamics of Polymeric Liquids*, 2nd ed.; Wiley: New York, 1987.

BM061039K